

## The Effects of the Content of NiO on the Microstructure and Photocatalytic Activity of the NiO/TiO<sub>2</sub> Composite Film

Guiyin ZHANG, Xinxin TANG, Xiuli CHEN, Wusheng ZHA \*

College of Material Science & Engineering, Xihua University, 999# Jin Zhou Rd. Jin niu District, Sichuan Province, Chengdu 610039 China

**crossref** <http://dx.doi.org/10.5755/j01.ms.24.4.19266>

Received 13 October 2017; accepted 25 December 2017

The NiO/TiO<sub>2</sub> composite films with the NiO content of 3 %, 5 %, 10 %, 13 %, 15 % and 20 % were prepared by mechanical coating technology and subsequent oxidation process. The composition and microstructure of the films were analyzed by X-ray Diffraction (XRD), scanning electron microscope (SEM), and energy dispersive spectroscopy (EDS). The photocatalytic activity was evaluated and the effects of the content of NiO on microstructure and photocatalytic activity of the films were studied. The results show that NiO particles are dispersed in the Ti coatings, and the NiO concentration in the inner layer of the coatings is higher than in the outer layer. With the addition of NiO in the NiO/Ti coating, the ductility is deteriorated and the thickness is reduced of the NiO/Ti coatings. The films with NiO/TiO<sub>2</sub>/Ti composite microstructure are obtained by the oxidation of NiO/Ti coatings. Photocatalytic efficiency of the films is obviously enhanced with the help of the p-n junction heterostructure in the NiO/TiO<sub>2</sub> films. The optimum content of NiO is about 13 %, and the degradation rate of methyl orange solution reaches the maximum value of 88.44 %.

**Keywords:** NiO content, NiO/TiO<sub>2</sub> composite films, mechanical coating technology, photocatalytic activity.

### 1. INTRODUCTION

Mechanical coating technology (MCT) is a novel film-forming method. The idea of MCT was from the mixing powders in powder metallurgy process, in which metallic adhesions on the surface of alumina balls in a pot of a planetary ball mill occur because of mechanical friction and abrasion. From that work, it was found that MCT is a simple and useful technique for forming a metallic film [1].

As a new film- and coating-preparation method, mechanical coating technology is widely used to prepare various coatings, such as metal coating [2, 3], amorphous composite metal coating and photocatalytic coating [4–6]. Consequently, the preparation of TiO<sub>2</sub> photocatalytic film by mechanical ball milling has become a hot topic.

Lu Yun successfully prepared TiO<sub>2</sub> photocatalytic films on the surface of Al<sub>2</sub>O<sub>3</sub> ceramic balls by MCT [7], and focused on improving the photocatalytic performance of the films. Particularly, the composite film of TiO<sub>2</sub>/NiO can significantly enhance the photocatalytic efficiency [8–10].

It is well known that titanium dioxide and nickel oxide are N-type and P-type semiconductors respectively, and the inner electric field may be constructed when TiO<sub>2</sub> couples with NiO [11, 12]. The inner electric field is helpful to separate the photogenerated electron-hole pairs on the surface of TiO<sub>2</sub>, thereby suppressing the recombination of electron-hole pairs and improving the photocatalytic performance.

In order to obtain the efficient photocatalytic films, the NiO/TiO<sub>2</sub> composite films with P-N junction mechanism have been prepared by MCT and subsequent oxidation process. In this paper, the effects of the content and distribution of NiO on the microstructure, composition and

the photocatalytic activity of composite films were investigated.

### 2. EXPERIMENTAL DETAILS

The powders, Ti powder (with the 99.5 % purity and an average diameter of 38 μm) and NiO powder, with the NiO content of 3 %, 5 %, 10 %, 13 %, 15 % and 20 % were poured into a grinding plot. ZrO<sub>2</sub> balls with an average diameter of 1mm were used as substrates, and the ball-to-powder weight ratio was maintained at 2.5:1. A planetary ball mill was used to perform the mechanical coating operation, and carried out with a rotation speed of 300 rpm for 15 h. The NiO/Ti coatings were oxidized in air at 773 K for 20 h to prepare NiO/TiO<sub>2</sub> composite films. The phase composition was analyzed by XRD with Cu-Kα radiation. The surface of the films was observed by the SEM(S-3400, secondary electron made), and the element distribution on the cross-section was analyzed by the energy dispersive spectrometer (EDS).

Each group of samples with 10 mg was poured into the 20 ml methyl orange solution (with the concentration of 10 mg/L), and then under the ultraviolet irradiation for 24 h. The spectrophotometer was used to measure the rate of concentration change of the methyl orange solution, the measured wavelength was set as 464 nm, which is near the peak of absorption spectrum of methyl orange solution. To ensure identical initial condition, the samples were pre-adsorbed by the methyl orange solution in the dark for 12 h. And a control group was provided to eliminate the experimental error caused by the spontaneous decomposition of methyl orange solution under the ultraviolet irradiation.

\* Corresponding author. Tel.: +8613688091585.  
E-mail address: 1434758301@qq.com (W. Zha)

### 3. RESULTS AND DISCUSSION

#### 3.1. Cross-sectional and surface morphologies of the samples

Fig. 1 shows the cross-sectional OM micrographs of the Ti coatings with different NiO content. The average thickness of the coatings without the addition of NiO is largest in all of the samples. The coating thickness gradually reduced with the increase of the content of NiO. The average thickness of the coatings with the NiO content of 0 %, 5 %, 13 %, and 20 % is about 75  $\mu\text{m}$ , 70  $\mu\text{m}$ , 65  $\mu\text{m}$  and 55  $\mu\text{m}$ , respectively.

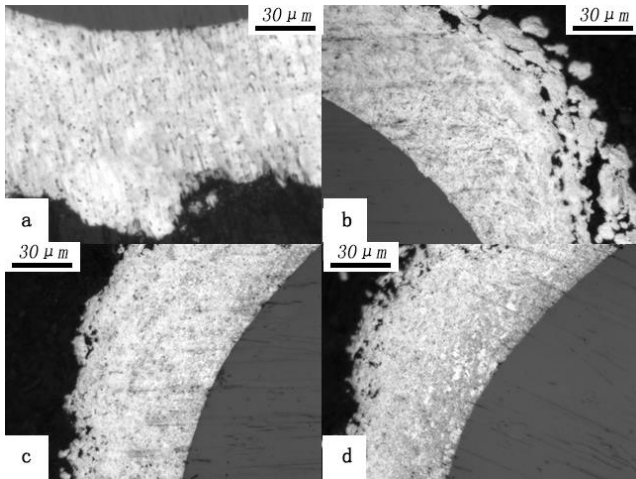


**Fig. 1.** Optical micrographs of the cross-section of Ti coatings with the NiO content of: a–0 %; b–5 %; c–13 %; d–NiO 20 %

Fig. 2 shows the surface SEM micrographs of the as-oxidized samples with the NiO content of 5 %, 13 % and 20 %. We can see that the surface particles are bonded with each other to form a flake due to the plastic deformation, and the flakes are stacked layer by layer to form a coating. As the increase of NiO content in the coatings, the size of the flakes on the coating surface is significantly reduced, and some isolated small size flakes appear on the surface of the coatings.

The NiO particles, which are hard particles, added in the matrix of metal titanium will result in the ductility deterioration of the coating materials. And the higher nickel oxide content, the more apparent ductility deterioration will become. The particles can not be easily cold-welded and bonded with each other due to the ductility deterioration of the coating materials, so that the average thickness of the coatings decreases. And the flat-shape particles are vulnerable to crack, and not to form large-sized flakes.

#### 3.2. Microstructure of the NiO/TiO<sub>2</sub> films

The cross-sectional micrograph of NiO/TiO<sub>2</sub> film with the NiO content of 20 % is shown in Fig. 3. The cross-section of the film is composed of bright-white phase and gray phase. The gray phase is dispersed in the bright-white phase. The element distribution of the cross-section of the film was analyzed by EDS, and the results are shown in Fig. 4. The concentration of titanium element of the bright-white area is higher than in the gray one, however, the concentration of nickel and oxygen element is lower than in

the gray one. It means that the gray area in the film is mainly nickel oxide, and the bright-white area is mainly metal titanium and its oxide.

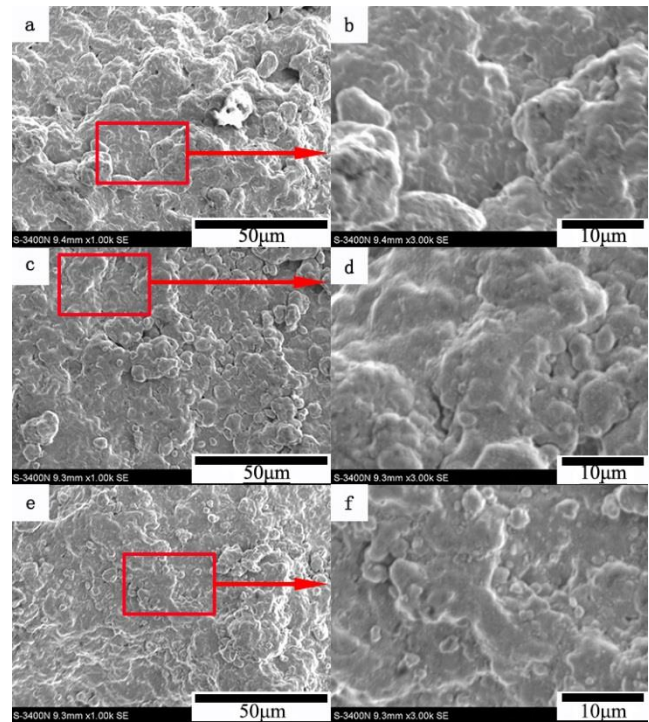


**Fig. 2.** SEM micrographs of the as-oxidized samples with the NiO content of: a–NiO 5 %; b–NiO 13 %; c–NiO 20 %

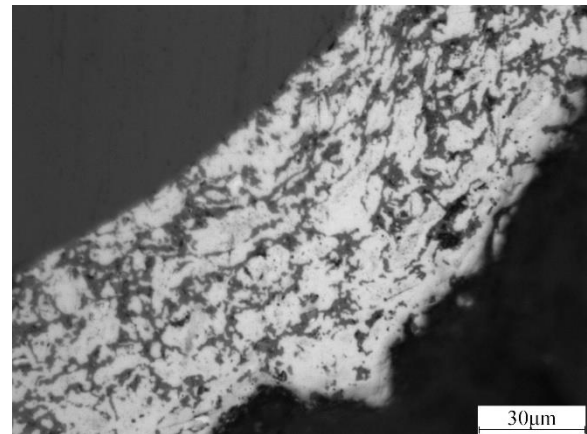


**Fig. 3.** Micrograph of cross-section of the composite film with 20% NiO

The NiO of the gray areas is unevenly distributed in the Ti matrix, and the concentration of NiO in the inner layer close to the ball is higher than that in the outer layer. In the initial stage of the coating deformation, Ti particles have a finer ductility so that it can be cold-welded to the surface of the grinding balls at a faster rate to form a continuous coating. The NiO particles can also be wrapped by titanium particles and cold-welded to the coating. With the extension of the milling time, the work hardening occurs in the Ti particles, which results in ductility deterioration of the coating materials, the difficulty increase of cold welding and the formation rate reduction of the continuous coatings. Only the Ti particles that rolled up a small number of NiO particles can continue to be deformed, preferentially to be attached and cold-welded on the surface of the coatings and

eventually to increase the coating thickness. Otherwise, the ductility of the Ti particles that rolled up a large number of NiO particles is worse than the former, so that, these Ti particles are more difficult to be cold-welded to the surface of the coatings. Finally, the deposition volume of the NiO is greatly reduced in the surface layer.

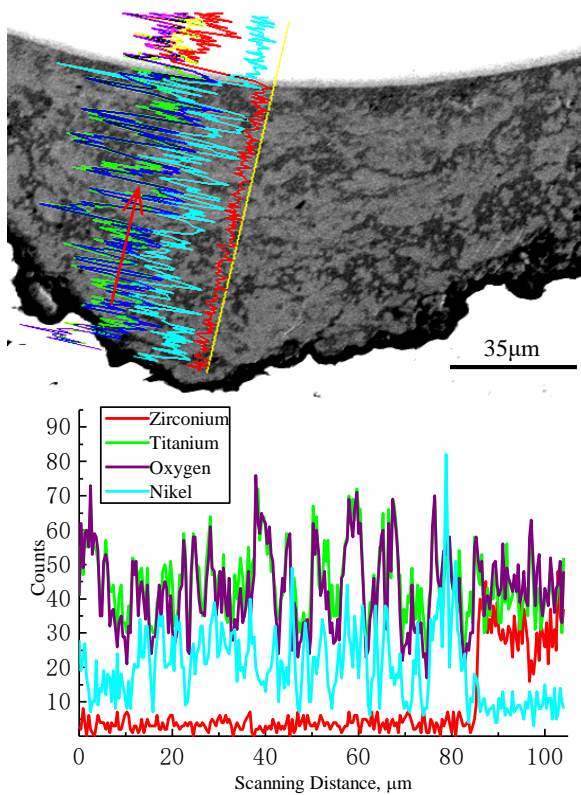


Fig. 4. EDS pattern of the composite film with 20% NiO

Fig. 5. shows the XRD pattern of the NiO/TiO<sub>2</sub> film with the NiO content of 13 %.

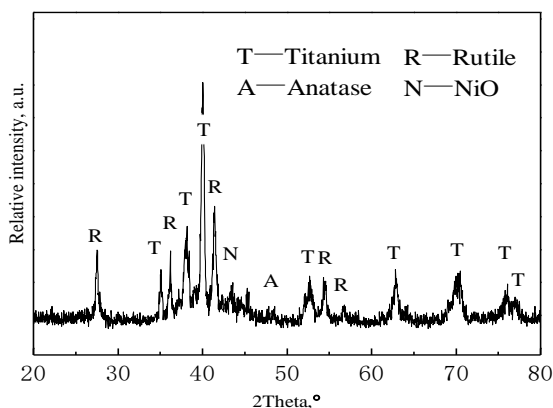


Fig. 5. XRD pattern of the composite film with 13 % NiO

In addition to the Ti and NiO diffraction peaks in the pattern, the rutile TiO<sub>2</sub> diffraction peaks with high intensity and the anatase TiO<sub>2</sub> diffraction peaks which the 2 θ is about 48° with the lower intensity appear. It means that the NiO/TiO<sub>2</sub>/Ti composite structure is prepared, and it contains rutile phase and anatase phase of TiO<sub>2</sub>, moreover, the concentration of the rutile TiO<sub>2</sub> is higher than the anatase TiO<sub>2</sub>.

### 3.3. Photocatalytic performance of the NiO/TiO<sub>2</sub> films

The samples with the different NiO content were poured into the methyl orange solution respectively, and then irradiated by UV-light for 24 h. Fig. 6 shows the degradation rates of methyl orange solutions at different irradiation time, and Fig. 7 shows the dependence of the 24 hour's degradation rate of methyl orange solution on the NiO content. In the case of the samples without the NiO, the degradation rate of the methyl orange solution is 73.26 %. With the addition of NiO, the degradation rate is significantly increased. The degradation rate of methyl orange solution reaches a peak of 88.44 %, of which the NiO content is about 13 %.

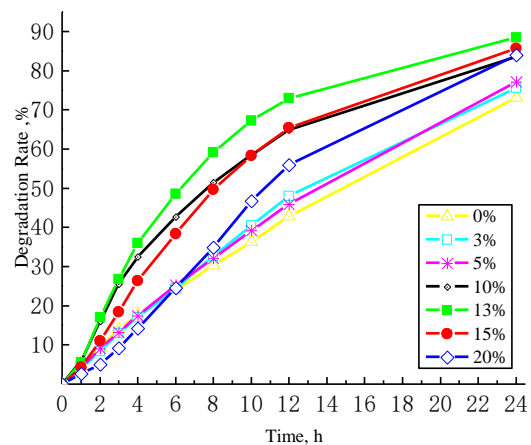


Fig. 6. Dependence of the photocatalytic time on the degradation rates of the methyl orange solutions

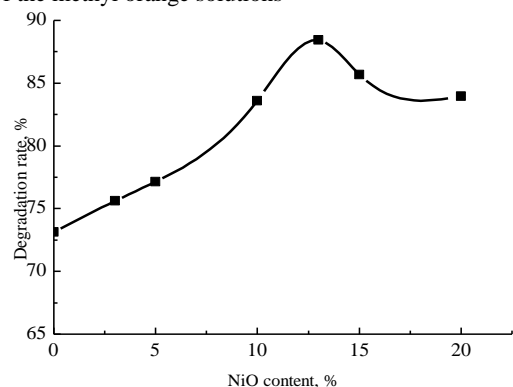


Fig. 7. Dependence of the 24 hour's degradation rate of methyl orange on the content of NiO

Ti particles and NiO particles are tightly compacted and combined by high-energy mechanical ball milling to form NiO/Ti coating. And the NiO/TiO<sub>2</sub> structure was obtained by oxidizing the titanium to the titanium dioxide at 773 K for 20 h. Although the diffraction peak intensity of Ti is very high in the composite film, the outermost film is a semiconductor layer composed of NiO and TiO<sub>2</sub> by oxidation sintering. The grains of the NiO and TiO<sub>2</sub> at their two-phase interface were closely combined to build a P-N heterojunction structure, and to create an inner electric field. The photogenerated electron-hole pairs at the surface of TiO<sub>2</sub> will be separated by the inner electric field. The holes flow to the negatively charged NiO region, and the electrons flow to positively charged TiO<sub>2</sub> region, which results in the significant improvement of the photocatalytic efficiency. As

a result, the degradation rate of methyl orange solution was improved with the addition of NiO in the photocatalytic film, and was enhanced with the further increase of the NiO content.

However, when the NiO content was beyond to 13 %, the content of titanium dioxide in the composite film was relatively reduced and the photocatalytic active component was diluted with the further increase of NiO, which results in the reduction of the photocatalytic activity of the composite films. Therefore, the optimum content of NiO is about 13 %, and the degradation rate of methyl orange solution reaches the maximum value.

#### 4. CONCLUSIONS

1. With the addition of NiO in the NiO/Ti coating, the ductility of the coating is deteriorated, and the particles can not be easily cold-welded and bonded with each other. That results in the reduction of the average thickness and the size of the flakes of the coating.
2. The NiO particles are dispersed in the Ti coating, and the concentration of NiO in the inner layer is higher than in the outer layer.
3. The NiO/Ti coating has been changed into the composite film with the structure of NiO/TiO<sub>2</sub>/Ti, and the rutile and a little anatase TiO<sub>2</sub> appears in the film by the heat oxidation at 773 K for 20 h.
4. The P-N junction was formed at the two-phase interface of NiO and TiO<sub>2</sub> due to the structure of NiO/TiO<sub>2</sub>/Ti in the film, which is helpful to improve the photocatalytic activity of the film under the UV irradiation. The optimum content of NiO is about 13 %.

#### REFERENCES

1. **Hao, L., Lu, Y., Sato, H., Asanuma, H.** Fabrication of Zinc Coatings on Alumina Balls from Zinc Powder by Mechanical Coating Technique and the Process Analysis *Powder Technology* 228 2012: pp. 337–384. <https://doi.org/10.1016/j.powtec.2012.05.056>
2. **Xinxin, T., Wusheng, Z., Guiyin, Z., Pengpeng, L., Jing, T.** The Effects of Oxidation Temperature on the Microstructure and Photocatalytic Activity of the TiO<sub>2</sub> Coating *Materials Science* 23 (2) 2017: pp. 103–107. <http://dx.doi.org/10.5755/j01.ms.23.2.15590>
3. **Hao, L., Yoshida, H., Takaomi, I., Lu, Y.** Preparation of Metal Coatings on Steel Balls Using Mechanical Coating Technique and Its Process Analysis *Coatings* 7 (4) 2017: pp. 53. <http://dx.doi.org/10.3390/coatings7040053>
4. **Lu, Y., Matsuzaka, K., Hao, L., Hirakawa, Y., Yoshida, H., Pan, F.S.** Photocatalytic Activity of TiO<sub>2</sub>/Ti Composite Coatings Fabricated by Mechanical Coating Technique and Subsequent Heat Oxidation *Materials Science in Semiconductor Processing* 16 (6) 2013: pp. 1949–1956. <https://doi.org/10.1016/j.mssp.2013.07.024>
5. **Takaya, S., Lu, Y., Guan, S., Miyazawa, K., Yoshida, H., Asanuma, H.** Fabrication of the Photocatalyst Thin Films of Nano-structured potassium Titanate by Molten Salt Treatment and Its Photocatalytic Activity *Surface and Coatings Technology* 275 2015: pp. 260–263. <https://doi.org/10.1016/j.surfcoat.2015.05.009>
6. **Guan, S., Hao, L., Lu, Y., Hiroyuki, Y., Asanuma, H.** Fabrication of Photocatalyst Composite Coatings of Cr-TiO<sub>2</sub> by Mechanical Coating Technique and Oxidation Process *Coatings* 5 (3) 2015: pp. 545–556. <http://dx.doi.org/10.3390/coatings5030545>
7. **Yoshida, H., Lu, Y., Nakayama, H., Hirohashi, M.** Fabrication of TiO<sub>2</sub> Film by Mechanical Coating Technique and Its Photocatalytic Activity *Journal of Alloys and Compound* 475 (1–2) 2009: pp. 383–386. <https://doi.org/10.1016/j.jallcom.2008.07.059>
8. **Bingbing, Z., Dafeng, Z., Zuoshuai, X., Pengfei, W., Xipeng, P., Xin, S., Shujuan, Y.** Synthesis of Ag<sub>2</sub>O/NaNbO<sub>3</sub> p-n Junction Photocatalysts with Improved Visible Light Photocatalytic Activities *Separation and Purification Technology* 178 2017: pp. 130–137. <https://doi.org/10.1016/j.seppur.2017.01.031>
9. **Xiaoju, W., Chang, Z., Chenggang, N., Lei, Z., Guangming, Z., Xuegang, Z.** Highly Enhanced Visible Light Photocatalytic Activity of CeO<sub>2</sub> Through Fabricating a Novel p-n Junction BiOBr/CeO<sub>2</sub> *Catalysis Communications* 90 2017: pp. 51–55. <https://doi.org/10.1016/j.catcom.2016.11.018>
10. **Zhangsheng, L., Biantao, W., Jinan, Niu., Peizhong, F., Yabo, Z.** BiPO<sub>4</sub>/BiOBr p-n Junction Photocatalysts: One-pot Synthesis and Dramatic Visible Light Photocatalytic Activity *Materials Research Bulletin* 63 2015: pp. 187–193. <https://doi.org/10.1016/j.materresbull.2014.12.020>
11. **Sharma, A., Lee, G.J.** Photocatalytic Reduction of Carbon Dioxide to Methanol Using Nickel-Loaded TiO<sub>2</sub> Supported on Activated Carbon Fiber *Catalysis Today* 298 2017: pp. 158–167. <https://doi.org/10.1016/j.cattod.2017.05.003>
12. **Rawool, S.A., Pai, M.R., Banerjee, A.M. Arya, A., Ningthoujam, R.S., Tewari, R., Rao, R., Chalke, B., Ayyub, P., Tripathi, A.K., Bharadwaj, S. R.** PN Heterojunctions in NiO:TiO<sub>2</sub> Composites with Type-II Band Alignment Assisting Sunlight Driven Photocatalytic H<sub>2</sub> Generation *Applied Catalysis B: Environmental* 221 2018: pp. 443–458. <https://doi.org/10.1016/j.apcatb.2017.09.004>